CORROSION RESISTANCE OF MECHANICALLY CLINCHED IF STEEL AND MG-3.0AL-1.0ZN-0.3MN-0.5ND-XLA (X=0.1, 0.2 AND 0.5) ALLOY

Ziadoon Tareq Mhawesh MHAWESH

2021
MASTER THESIS
METALLURGICAL AND MATERIALS ENGINEERING

Thesis Advisor
Dr. İsmail Hakkı KARA

CORROSION RESISTANCE OF MECHANICALLY CLINCHED IF STEEL AND MG-3.0AL-1.0ZN-0.3MN-0.5ND-XLA (X=0.1, 0.2 AND 0.5) ALLOY

Ziadoon Tareq Mhawesh MHAWESH

T.C.
Karabuk University
Institute of Graduate Programs
Department of Metallurgical and Materials Engineering
Prepared as
Master Thesis

Thesis Advisor
Assist. Prof. Dr. İsmail Hakkı KARA

KARABUK
December 2021

I certify that in my opinion the thesis submitted by Ziadoon Tareq Mhawesh MHAWESH titled "CORROSION RESISTANCE OF MECHANICALLY CLINCHED IF STEEL AND MG-3.0AL-1.0ZN-0.3MN-0.5ND-XLA (X=0.1, 0.2 AND 0.5) ALLOY" is fully adequate in scope and in quality as a thesis for the degree of Master of Science.

Assist. Prof. Dr. İsmail Hakkı KARA .....
Thesis Advisor, Department of Metallurgical And Materials Engineering

This thesis is accepted by the examining committee with a unanimous vote in the Department of Metallurgical and Materials Engineering as a Master of Science thesis. December 24, 2021

Examining Committee Members (Institutions)	Signature
Chairman : Prof.Dr. Mustafa ACARER (SU)	.....
Member : Prof.Dr. Hayrettin AHLATCI (KBU)	.....
Member : Assist.Prof.Dr. İsmail Hakkı KARA (KBU)	.....

The degree of Master of Science by the thesis submitted is approved by the Administrative Board of the Institute of Graduate Programs, Karabuk University.

Prof. Dr. Hasan SOLMAZ .....
Director of the Institute of Graduate Programs

"I declare that all the information within this thesis has been gathered and presented in accordance with academic regulations and ethical principles and I have according to the requirements of these regulations and principles cited all those which do not originate in this work as well."

Ziadoon Tareq Mhawesh MHAWESH

ABSTRACT

M. Sc. Thesis

CORROSION RESISTANCE OF MECHANICALLY CLINCHED IF STEEL AND MG-3.0AL-1.0ZN-0.3MN-0.5ND-XLA (X=0.1, 0.2 AND 0.5) ALLOY

Ziadoon Tareq Mhawesh MHAWESH

Karabük University
Institute of Graduate Programs
The Department of Metallurgical and Materials Engineering

Thesis Advisor:
Assist. Prof. Dr. İsmail Hakkı KARA
December 2021, 43 pages

Magnesium alloys are recommended to utilize in structural section of automotive industry because of their low-density value of 1.74 g/cm ^{3} which enable to decreasing of fuel consumption. However, the application of Mg alloys is very limited due to their low formability and moderate strength properties. The steels are used on many parts of automotive. IF steel that is known as excellent mechanical properties which contributes to using in many automobile parts such as longitudinal beams, cross members, B-pillars as well as skin parts. High strength IF steels are unmatched in deep drawing and mechanical strength. IF steels gain solid melt hardening in ferrite with manganese, silicon, and phosphorus. Besides their mechanical strength, they have good fatigue and impact resistance. The mechanical clinching method is a process without the need for additional material. Thanks to plastic deformation, thin sheet metallic materials are joined. To enhance the using application of Mg alloys in automobile parts, the mechanical clinching method is available due to steel- Mg joining is possible. In this study, IF steel sheets of 0.6 mm

were joined by mechanical clinching with AZ31B Mg sheets containing Neodymium and Lanthanum. Then the corrosion resistance of clinched specimens was investigated by cross-section with potentiodynamic and immersion corrosion tests in 3.5% NaCl solution at 25°C. The results demonstrated that the rare earth added AZ31B Mg alloys can utilized to diminish corrosion rate in condition of both Nd and La amount is specific.

Key Words : AZ31B, Nd, La, corrosion, Mechanical Clinching.

Science Code : 91513

ÖZET

MEKANİK OLARAK PERÇİNLENMİŞ ÇELİK VE MG-3.0AL-1.0ZN-0.3MN-0.5ND-XLA (X=0.1, 0.2 VE 0.5) ALAŞIMININ KOROZYON DİRENCİ

Ziadoon Tareq Mhawesh MHAWESH

Karabük Üniversitesi

Lisansüstü Eğitim Enstitüsü
Metalurji ve Malzeme Mühendisliği Anabilim Dalı

Tez Danışmanı:
Dr. Öğretim Üyesi İsmail Hakkı KARA

Aralık 2021, 43 sayfa

Magnezyum alaşımlarının yakıt tüketiminin azalmasını sağlayan 1,74 g/cm3 gibi düşük yoğunluk değerleri nedeniyle otomotiv endüstrisinin yapısal bölümünde kullanılması tavsiye edilir. Bununla birlikte, düşük şekillendirilebilirlik ve orta mukavemet özelliklerinden dolayı Mg alaşımlarının uygulaması çok sınırlıdır. Çelikler otomotivin birçok yerinde kullanılmaktadır. Uzunlamasına kirişler, traversler, B sütunları gibi birçok otomobil parçasının yanı sıra kaplama parçaları gibi birçok otomobil parçasında kullanılmasına katkıda bulunan mükemmel mekanik özellikler olarak bilinen IF çeliği. Yüksek mukavemetli IF çelikleri, derin çekme ve mekanik mukavemette eşsizdir. IF çelikleri, manganez, silikon ve fosfor ile ferrit içinde katı eriyik sertleşmesi kazanır. Mekanik mukavemetlerinin yanı sıra iyi yorulma ve darbe direncine sahiptirler. Mekanik perçinleme yöntemi ek malzemeye ihtiyaç duyulmayan bir işlemdir. Plastik deformasyon sayesinde ince sac metal malzemeler birleştirilir. Otomobil parçalarında Mg alaşımlarının kullanımını geliştirmek için, çelik-Mg birleştirmesi mümkün olduğundan mekanik perçinleme yöntemi mevcuttur. Bu çalışmada 0.6 mm IF çelik saclar, Neodimyum ve Lantan içeren AZ31B Mg saclar ile mekanik perçinleme ile birleştirilmiştir. Daha sonra

perçinlenen numunelerin korozyon direnci, potantiodinamik ve daldırma korozyon testleri ile %3.5'lik NaCl çözeltisi içinde 25°C'de kesit alınarak incelenmiştir. Sonuçlar, nadir toprak katkılı AZ31B Mg alaşımlarının hem Nd hem de La miktarının spesifik olması durumunda korozyon hızını azaltmak için kullanılabileceğini göstermiştir.

Anahtar Kelimeler : AZ31B, Nd, La, korozyon, Mekanik Perçinleme.

Bilim Kodu **:** 91513

ACKNOWLEDGMENT

At first and before everyone I would like to thank God who helped me to complete this study. After that I would like to thank my father and mother who supported me, and I would like to give thanks to my advisor, Assist. Prof. Dr. İsmail Hakkı KARA, for his great interest and assistance in preparation of this thesis. Also, I would like to give thanks to Dr. Metin ZEYVELİ because he has supported me to complete the mechanic clinching process.

In addition to, I would like to thank the KBU-BAP unit for supporting this study with BAP Project No: FYL-2020-2254 by Karabuk University Scientific Research Projects Coordinator ship.

CONTENTS

Page

Page

LIST OF FIGURES

Page

LIST OF TABLES

Page

SYMBOLS AND ABBREVITIONS INDEX

SYMBOLS

Corr. : Corrosion

m : mass of matter whose phase changes

g : gram

ABBREVITIONS

NaCl : Sodium chloride

XRF : X-ray fluorescence

SEM : Scanning Electron Microscope

PART 1

INTRODUCTION

Metals make up about 75% of automobile materials. plastics, composite materials, and ceramics complete the rest. The amount of steel used is around 50%, but magnesium is around 0.3%. Steels have a great utilization rate. because it has strength, resource ability and recycling properties. As metallic materials, aluminum and magnesium are preferred to absorb impacts and reduce weight.

1.1. MG ALLOYS

There is intense interest in using magnesium alloys in automobile parts to reduce fuel consumption in automobiles. AZ31, AZ91, AM60 and AM50 alloys are mostly preferred for die casting, room temperature strength and ductility. AZ31 Mg alloys are widely used as sheet material [1]. These alloys are mostly used in some building materials at room temperature environments. The use of magnesium in automobile body, structure and engine parts is increasing. however, their usage rates are low due to their low strength and bonding properties. Mg alloys in the form of plates, sheets and foils are produced by the rolling method [2]. Magnesium sheet materials are sufficient for automotive applications due to their mechanical properties. wrought Mg-Mn alloys are not suitable for heat treatment. Its mechanical properties are low, but its welding capabilities and corrosion resistance are high. They are suitable for welding applications. Mg-Al-Zn alloys (AZ10A, AZ31B, AZ61A, AZ80A) are suitable for heat treatment and can be harden by precipitation hardening [3]. strength and welding capabilities are good. some application areas aircraft fuselage, computer cases, speaker cones, super-plastic sheets, extruded plates, sheets, and sections of moderate cost, rolled sheets and plates, photoengraving sheets. Wrought Mg-Zn-Zr-Th alloys (ZK10A, ZK20A, ZK60A, HM13A and HM31A) are heat treatable and

have high strength. Zr is used as grain refiner. their strength is high, but their welding ability and shaping ability are low [4].

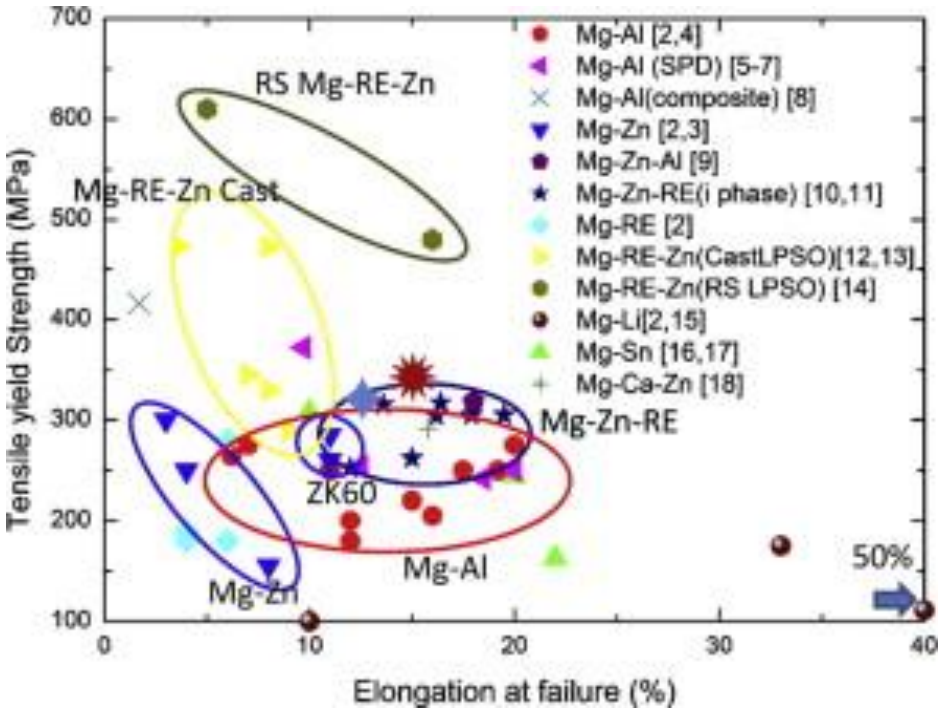

Figure 1. 1.Mg alloys and their mechanical properties [4].

1.1.1. AZ31B Mg Sheets

AZ31B Mg sheets have been collected excellent interest in using application of automobile parts due to their excellent properties such as high specific strength and low density. The alloying elements of Al, Zn and Mn enhance the properties of strength, toughness, and corrosion, respectively. Zn is detrimental when it is amount is higher than standards. To diminish micro porosity of Mg alloys, rare earth elements is utilized as well as Zr can be useful to grain refinement. Ag and Cu can be chosen to enhance high temperature and creep properties of Mg alloys. Mg is lighter than aluminum as 35%. To develop the absorption properties of Mg-Al-Zn alloy, the Al amount could add under 5%. The production of Mg alloys is accomplished by casting methods of high pressure die and sand mold casting [5].

1.2. CLINCHING METHODS

Clinching initiates advanced opportunities of joining lightweight sheet materials in the building field of lightweight designs [6].

1.1.3. Mechanical Clinching

The mechanical riveting method is a process without the need for additional material. Thanks to plastic deformation, thin sheet metallic materials are joined. The process can be done at room temperature or at high temperatures, depending on the material type. Some advantages of the mechanical riveting method are as follows [7]:

- reduced defragmentation time (less than one second)
- reduced cost (no need for additional materials such as screws)
- reduced machine cost
- No drilling is required before joining.
- Different materials can be combined.
- Due to work hardening, an increase in the hardness of the metal is observed.

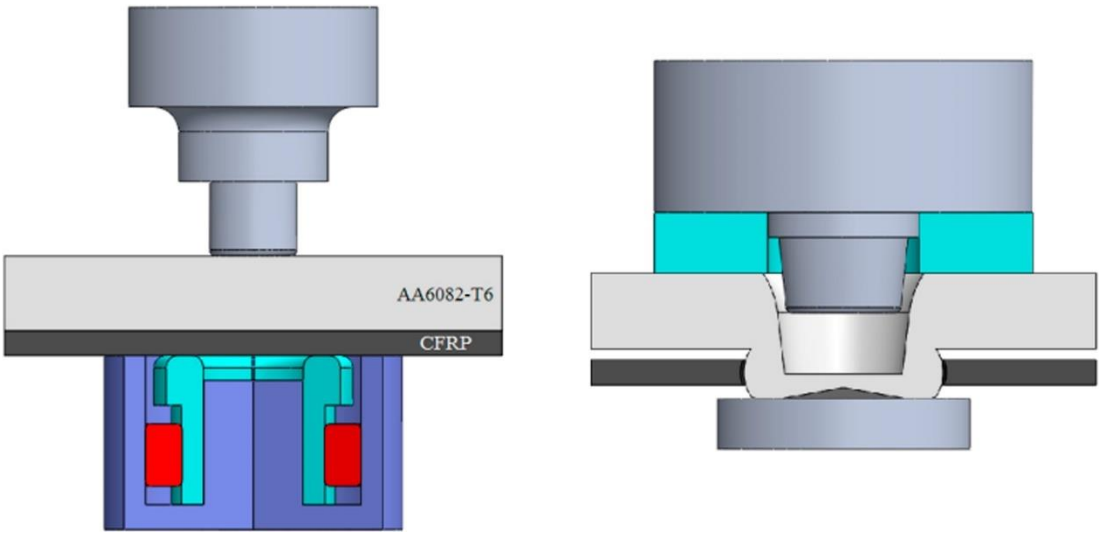

Figure 1.2. Clinhing process [7].

1.1.4. Hybrid Joining

The combination of two or more joining techniques can be attained by single techniques of Hybrid joining. The improvement of mechanical properties can be achieved by using of Hybrid joining better than adhesive bonding, riveting and others [7].

Figure 1.3. Metal–composite specimen produced by hybrid joining [7].

1.1.4. Hydro-Clinching

Hydro-clinching includes hydroforming and clinching that is knowns as new clinching method. In hydro-clinching, a high-pressure fluid is employed as the die and this exchange enhances the range of functions for clinching to areas not coated by accepted clinching approaches. The favor of hydro-clinching is the reduction of the quantity of processing stages and the advanced arrangement opportunities [8].

1.1.5. Injection Clinching

The industry of transportation contains applications including multi-material structures have attained many considerable impacts in the field of clinching. Injection clinching is constructed on staking, adhesive bonding and injection molding which enables polymer-metal joining by spot anchoring [8].

1.3. THE USING OF MG ALLOYS IN CLINCHING PROCESS

Availability of light magnesium alloys has contributed to more events for weight reduction in transport system segments. A qualification for the lengthy use of these materials is the availability of ways to combine components. widely suitable and offers maximum use materials under employed loads. Homogeneous joining of Mg

components can be attained by clinching and with other metals. The formability is limited for Mg alloys due to the anisotropic behavior of structure of hexagonal crystal at lower temperatures than 220 °C. The rising temperature of clinching process enhances the joining capability of Mg alloys. Before process the location of clinching point is heated by induction resistance that contributes to high-quality joining. The beneficial of flat clinching method enables excellent capability to join of Mg alloys. A die containing a flat anvil is utilized to flat clinching process [8].

1.3. APPLICATION MECHANICAL CLINHING

The mechanical clinching has been placed on different industry application such as automotive, metallic furniture, building sector, electricity and electronic equipment and Appliance and HVAC such as washing machines, refrigerators, hot water boilers, dishwashers, micro-wave ovens, stoves, solar collectors, air conditioners, heat exchangers [2].

PART 2

EXPERIMENTAL STUDIES

The experimental studies include the casting of materials, homogenization after casting, hot rolled to obtain Mg sheets and mechanical clinching as well as corrosion tests containing potentiodynamic and immersion.

2.1. CASTING

AZ31, AZ31+0.5Nd+0.5La, AZ31+0.5Nd+0.25La and AZ31+0.5Nd+0.1La alloys were produced by induction melting method (see Figure 2.1) and the casting parameters is similar with our earlier study [9]. The chemical content of the compounds produced in the KBU Margem XRF Laboratory was examined (See Table 2.2). 7115 quality IF steel (0.06 C Max. 0.025 Pmax. 0.025 Smax. 0.35 Mn max. 0.085-0.095 Ti) was supplied from Erdemir Iron and Steel Factory.

Figure 2. 1. Induction furnace

Table 2. 1. Chemical composition of produced Mg alloys

Materials	Al	Mn	Zn	Nd	La	Mg
AZ31	3.62	0.11	1.18	-	-	Bal.
AZ31-0.5Nd-0.1La	3.01	0.27	0.95	0.48	0.11	Bal.
AZ31-0.5Nd-0.2La	2.92	0.15	0.91	0.49	0.23	Bal.
AZ31-0.5Nd-0.5La	2.88	0.25	0.87	0.45	0.54	Bal.

2.2. HEAT TREATMENT

The produced alloys were homogenized heat treated in a heat treatment furnace at 400°C for 24 hours (see Figure 2.2).

Figure 2. 2. The heat treatment furnace.

2.3. ROLLING

Using the hot conventional flat rolling method (see Figure 2.3), sheets with a wall thickness of 1.5 mm were produced from casting billets with an initial wall thickness of 6 mm at a rolling speed of 4.7 m/min at 400°C.

Figure 2. 3. Hot rolling device

2.4. JOINING PROCESS

The produced Mg alloys were successfully combined with IF steel with a wall thickness of 0.6 mm, which was supplied from Erdemir Iron and Steel Factory, by using a mechanical riveting device.

2.5. MICROSTRUCTURAL STUDIES

To examine the sectioned microstructures of the combined materials, firstly the samples were embedded in cold bakelite. Bakelite embedded specimens were cut using discotane. After sanding and polishing processes, etching was done using picral solution. The grains, grain boundaries and secondary phases were examined in terms of shape-size-distribution using scanning electron microscopy.

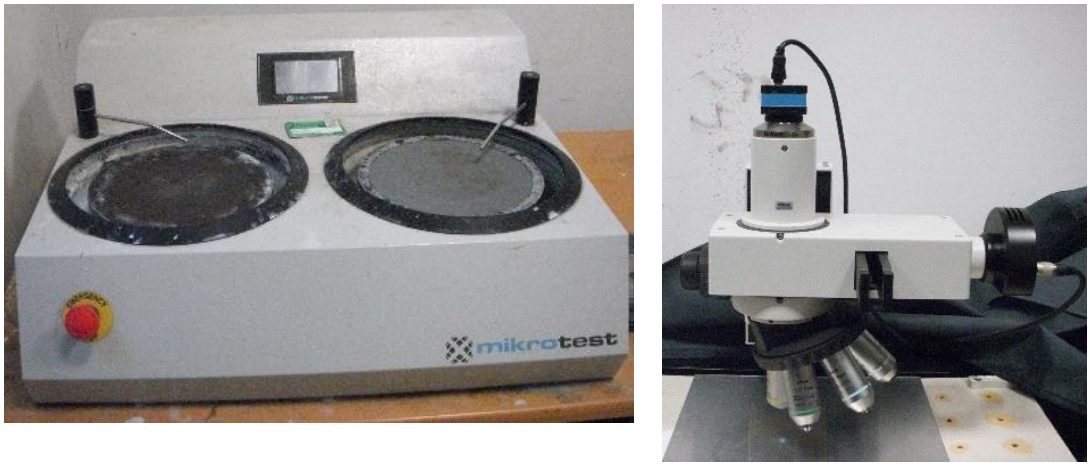

(a) (b)

Figure 2. 4. The devices of microstructural studies a) grinding and polishing b) optical microscopy.

2.6. POTENTIODYNAMIC CORROSION TESTS

Before the potentiodynamic test, the samples were wrapped with copper wire and embedded in cold bakelite. The corrosion resistance of the confluent samples along the section was measured in 3.5% NaCl solution.

Figure 2. 5. Potentiodynamic corrosion control unity.

2.7. IMMERSION CORROSION TESTS

Immersion corrosion tests were performed in 3.5% NaCl solution for 4,8 and16 hours.

Figure 2. 6. Immersion test method

PART 3

RESULTS AND DISCUSSION

3.1. MICROSTRUCTURE PROPERTIES

3.1.1. Scanning Electron Microscopy

3.1.1.1. Hot Rolled Alloys

EDS analysis was carried out to determination of elemental distribution inside secondary phases and matrix. Mg-Al-Mn, Al-Mn-Zn, Al-Mn, Mg-Al-Zn rich secondary phases were captured by EDS on the AZ31B alloy sheet (see Figure 3.1).

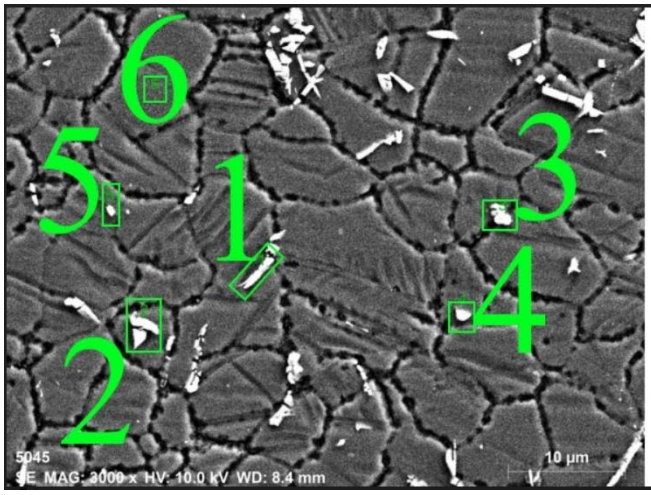

Mass percent (%)

Spectrum	Mg	Al	Mn	Zn
1	78.29	13.11	7.97	0.63
2	35.84	42.12	10.56	11.47
3	5.93	51.35	36.70	6.02
4	53.43	28.42	4.06	14.09
5	29.49	52.68	2.19	15.65
6	94.09	2.44	0.80	2.67
Mean value:	49.51	31.69	10.38	8.42
Sigma:	32.61	20.73	13.40	6.21
Sigma mean:	13.32	8.46	5.47	2.54

Figure 3. 1. Point EDX of matrix and secondary phases was obtained from AZ31B.

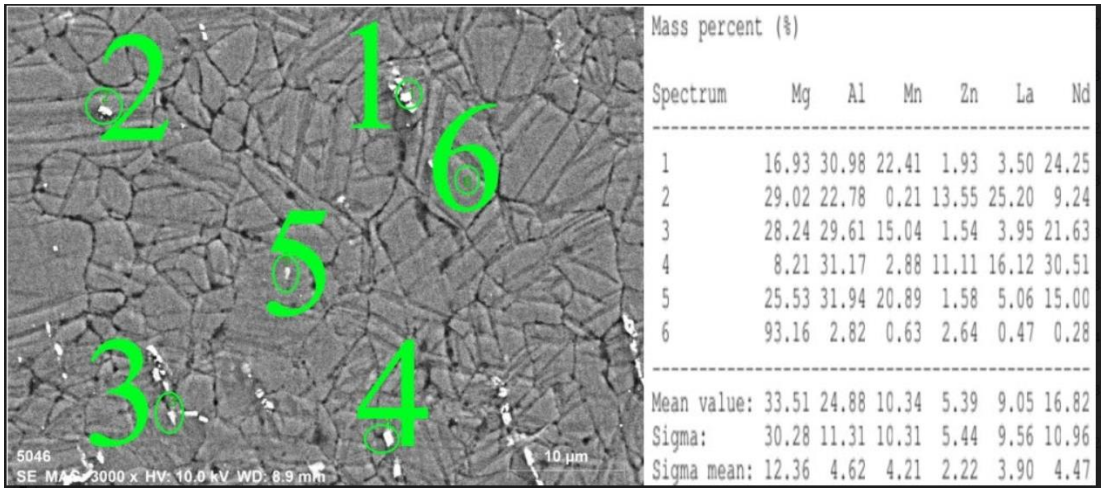

Figure 3. 2. Point EDX of matrix and secondary phases was obtained from AZ31B-0.5Nd-0.1La.

AZ31B-0.5Nd-0.1La alloy sheet contains the Al-Mn-Nd, Al-Zn-La, Al-Mn-Nd, Al-Zn-La-Nd, Al-Mn-Nd rich secondary phases which mostly distributed on the grain boundaries (see Figure 3.2).

The enlarged secondary phases occupied the grains boundaries of AZ31B-0.5Nd-0.2La alloy sheet as well as finer small particles was placed on grain boundaries with direction to rolling way. Moreover, Al-Mn-Nd and Al-La-Nd rich secondary phases is determined (see Figure 3.3).

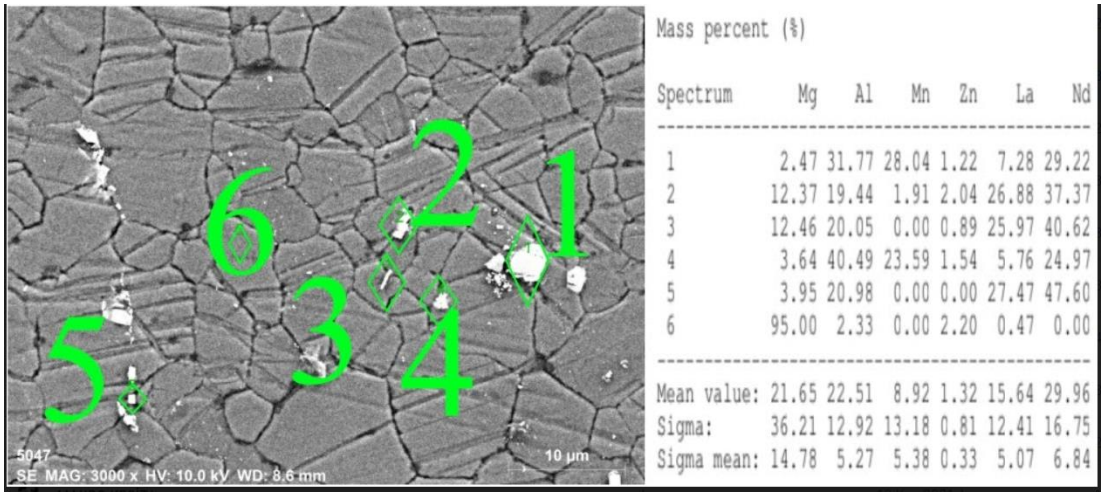

Figure 3. 3. Point EDX of matrix and secondary phases was obtained from AZ31B-0.5Nd-0.2La.

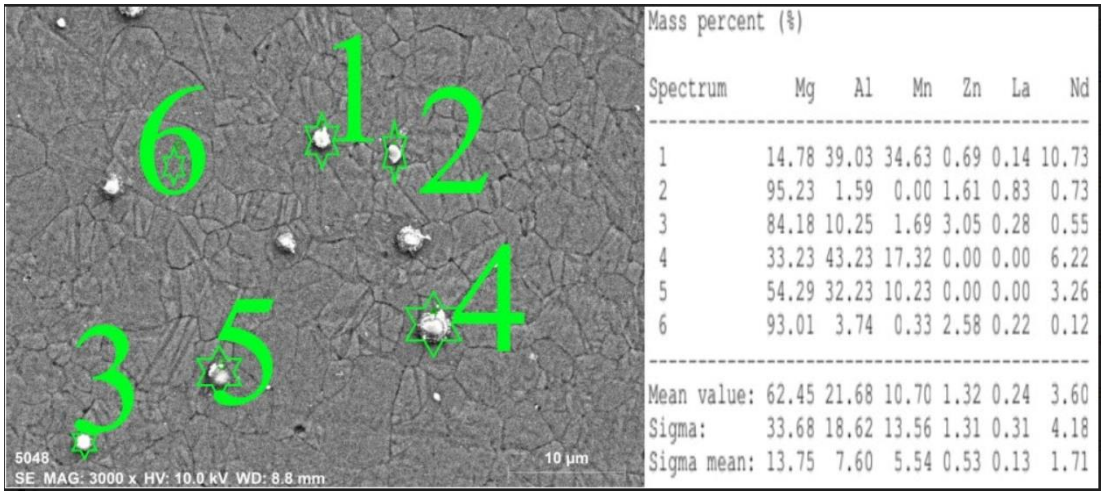

Mass percent (%)

Spectrum	Mg	Al	Mn	Zn	La	Nd
1	14.78	39.03	34.63	0.69	0.14	10.73
2	95.23	1.59	0.00	1.61	0.83	0.73
3	84.18	10.25	1.69	3.05	0.28	0.55
4	33.23	43.23	17.32	0.00	0.00	6.22
5	54.29	32.23	10.23	0.00	0.00	3.26
6	93.01	3.74	0.33	2.58	0.22	0.12
Mean value:	62.45	21.68	10.70	1.32	0.24	3.60
Sigma:	33.68	18.62	13.56	1.31	0.31	4.18
Sigma mean:	13.75	7.60	5.54	0.53	0.13	1.71

Figure 3. 4. Point EDX of matrix and secondary phases was obtained from AZ31B-0.5Nd-0.5La.

AZ31B-0.5Nd-0.5La alloy sheet includes oval shaped Al-Mn-Nd, Mg-Al and Al-Mn rich secondary phases which were formed on the grain boundaries (see Figure 3.4).

3.1.1.2. Clinched Alloys

The SEM micrographs of clinched IF steel sections are illustrated in Figure 3.5. S1 presents the undeformed grains. S2 section containing up and down locations shows rotated grains based on the deformation direction during clinching. S3 section displays fully deformed grains elongated to parallel to die.

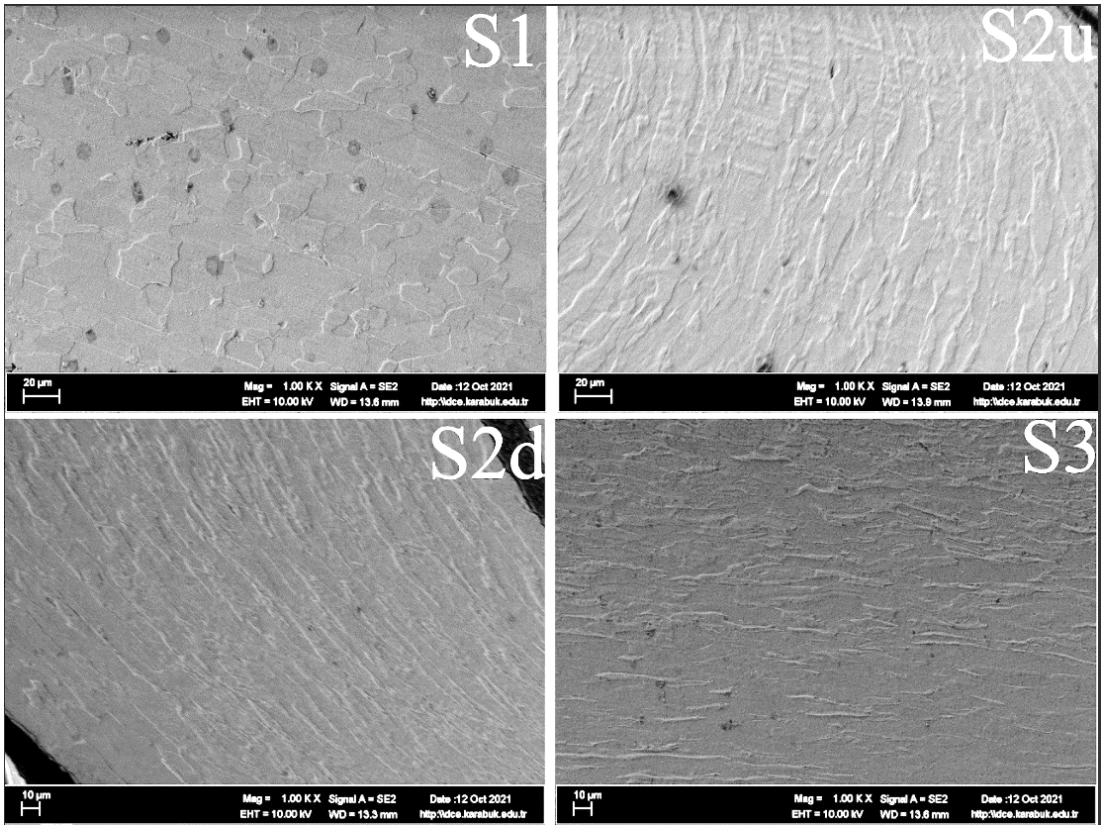

Figure 3. 5. SEM micrographs of clinched IF steel.

The SEM micrographs of clinched AZ31B sections are illustrated in Figure 3.6. S1 presents the undeformed grains consisting of twins. S2 section containing up and down locations shows rotated grains based on the deformation direction during clinching. S3 section displays fully deformed grains elongated to parallel to die. Moreover, the secondary phases became finer and agglomerated grain boundaries in the S2 region.

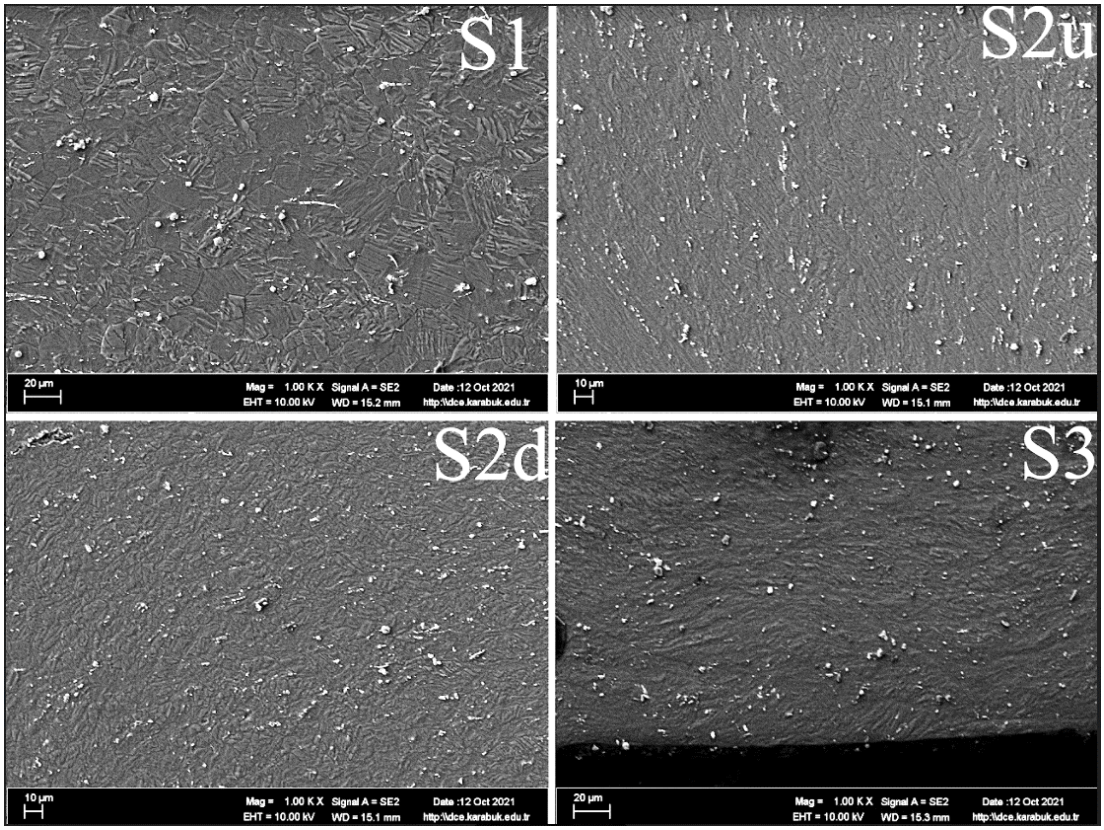

Figure 3.6. SEM micrographs of clinched AZ31B.

The grains on the location of S2 of AZ31B-0.5Nd-0.1La. was less rotated than AZ31B during clinching process. Moreover, S1 region shows twins dominated grains and oval and acicular shaped secondary phases distributing on the matrix and grain boundaries. Further, S3 region of deformed AZ31B-0.5Nd-0.1La by clinching demonstrates denser secondary phases volumetrically (see Figure 3.7).

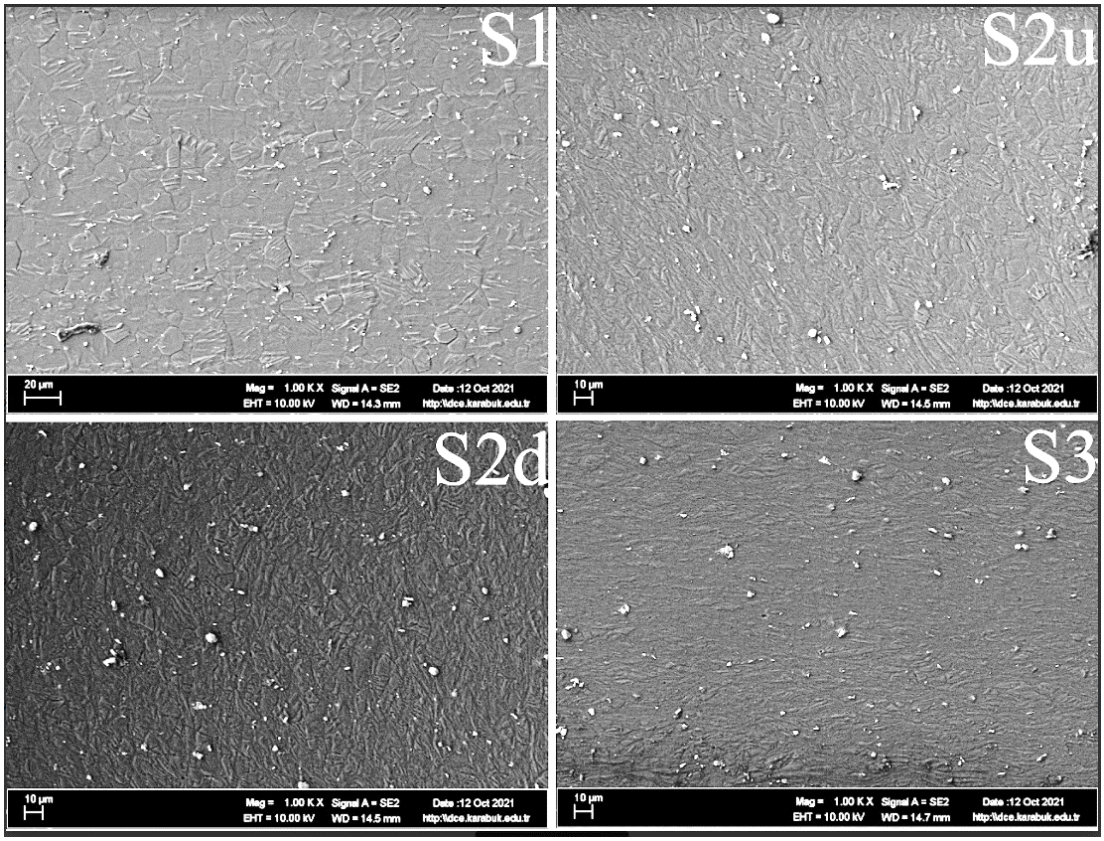

Figure 3.7. SEM micrographs of clinched AZ31B-0.5Nd-0.1La.

Deformed AZ31B-0.5Nd-0.2La alloy sheet illustrates homogeneously formed columnar like shaped secondary phases on the location of S2u. Moreover, fiber like secondary phases mostly introduced on the S2u location. However, the rotated grains are presented by the S2d location of AZ31B-0.5Nd-0.2La alloy sheet. S3 location is different from deformed AZ31Band of AZ31B-0.5Nd-0.1La alloy sheet because of the some grains were rotated to perpendicular angle through die direction which is confirmed by especially the upside grains of S3 region (see Figure 3.8).

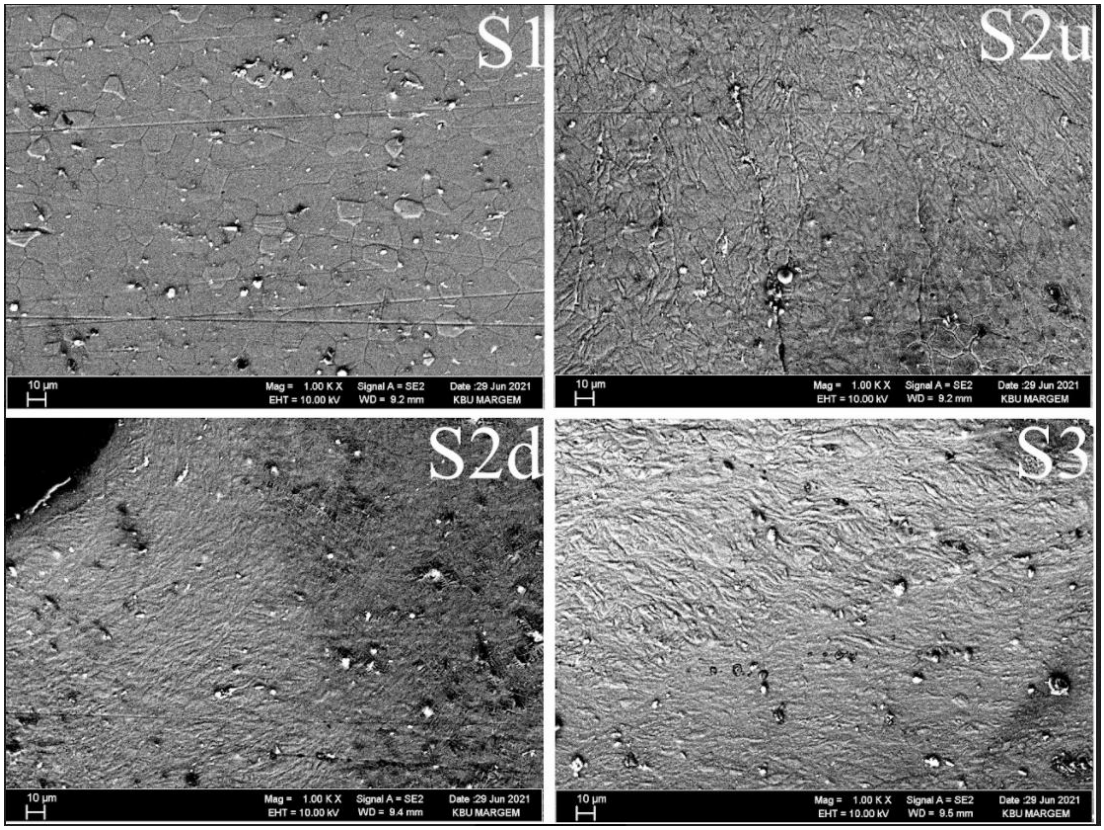

Figure 3.8. SEM micrographs of clinched AZ31B-0.5Nd-0.2La.

S1 location of AZ31B-0.5Nd-0.5La is similar with the Mg alloy sheets. However, the obeying of grains to rotation direction is very limited on the S2u location, where the elongated very thin and thick grains were formed (see Figure 3.9).

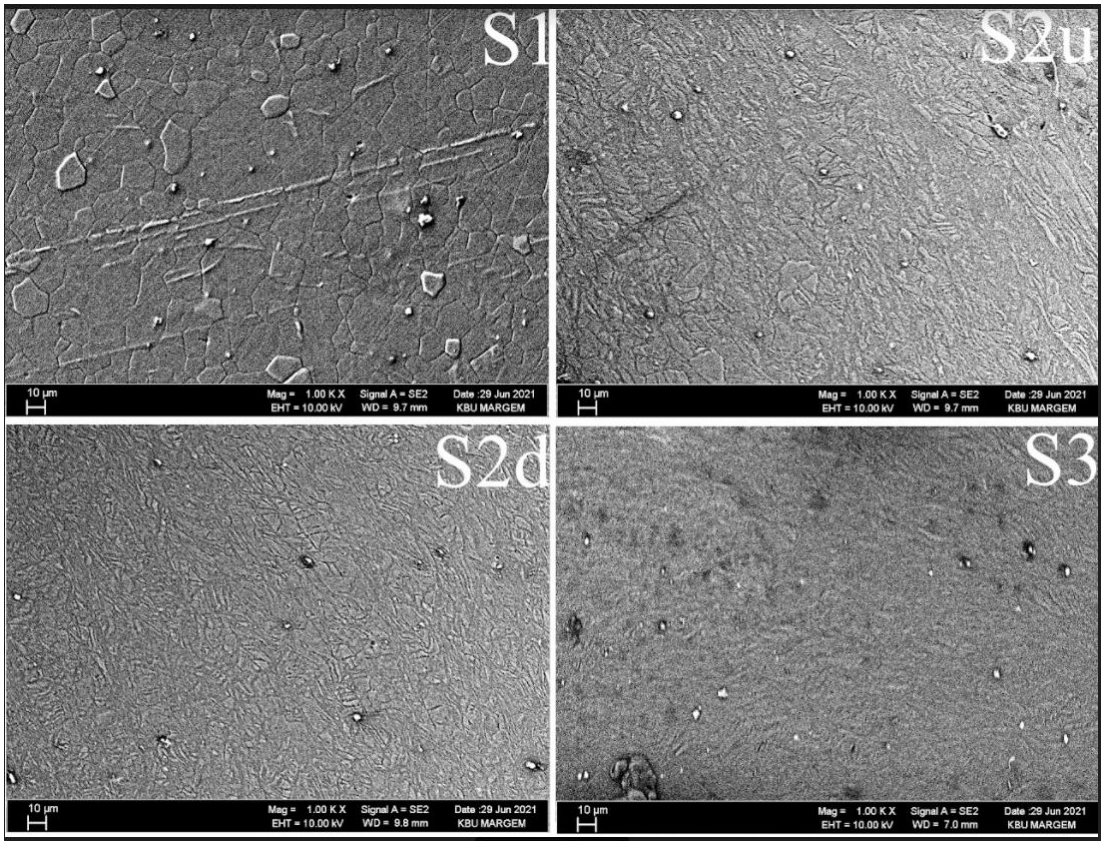

Figure 3.9. SEM micrographs of clinched AZ31B-0.5Nd-0.5La.

3.1.2. POTENTIODYNAMIC CORROSION

The potentiodynamic corrosion test results are given in Table 3.1. As seen from Table 3.1, the corrosion rate of locations of IF-AZ31B joint is ordered in the following S1>S2>S3. However, the corrosion rate of regions of IF-AZ31B-0.5Nd-0.1La is measured as S3>S1>S2. IF-AZ31B-0.5Nd-0.2La joint shows the corrosion rate in the order as S2>S1> S3. IF-AZ31B-0.5Nd-0.5La joint presents the corrosion rate like that order S1>S3>S2.

Table 3. 1. Potentiodynamic Corrosion test results.

Joined Materials and Sections	Ecorr(mV)	icorr(A/cm2)	corr rate(mpy)
IF-AZ31-S1	-1170	0,0178	3670
IF-AZ31-S2	-1410	0,0137	2820
IF-AZ31-S3	-1290	0,0127	2620
IF-AZ31-0.5Nd-0.1La –S1	-1290	0,00542	1110
IF-AZ31-0.5Nd-0.1La –S2	-1340	0,00504	1040
IF-AZ31-0.5Nd-0.1La –S3	-1390	0,00757	1560
IF-AZ31-0.5Nd-0.2La –S1	-1310	0,0135	2780
IF-AZ31-0.5Nd-0.2La –S2	-1350	0,605	124900
IF-AZ31-0.5Nd-0.2La –S3	-990	0,0484	989
IF-AZ31-0.5Nd-0.5La –S1	-1330	711	14740
IF-AZ31-0.5Nd-0.5La –S2	-1140	0,00592	1220
IF-AZ31-0.5Nd-0.5La –S3	-1180	0,0191	3930

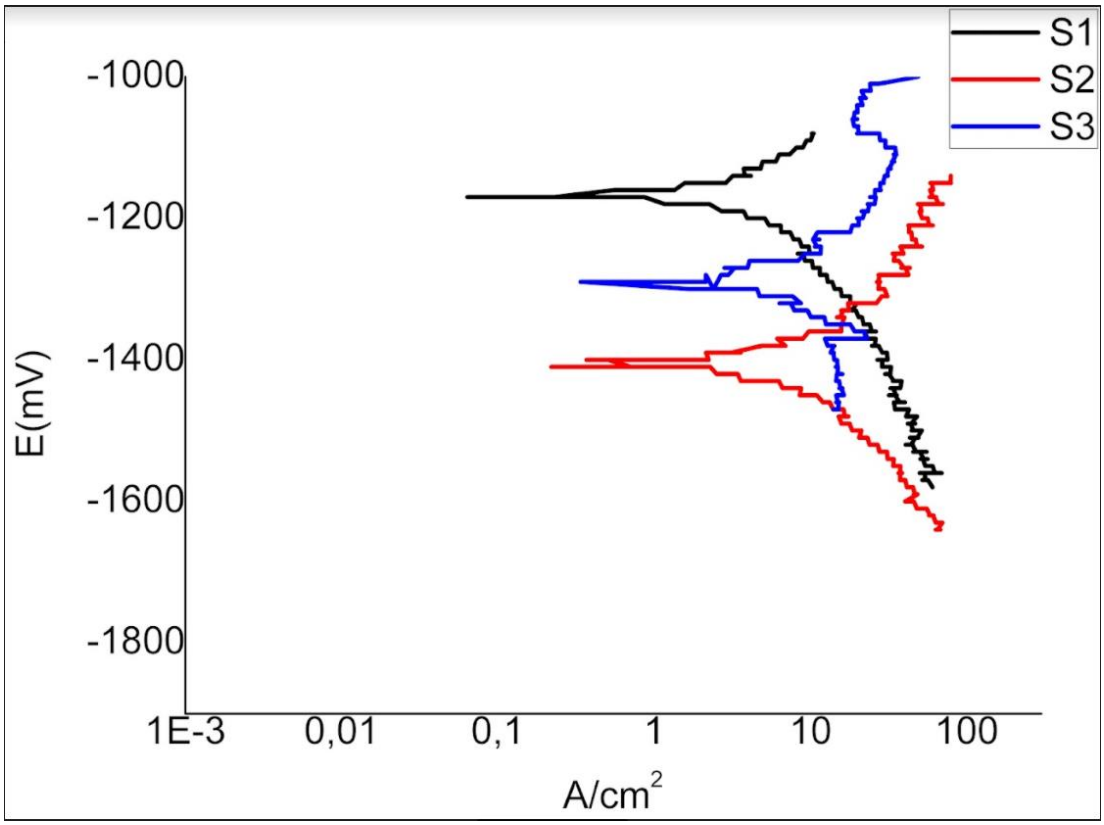

Figure 3. 10. Potentiodynamic Tafel curves obtained from S1, S2 and S3 sections of clinched IF-AZ31B

The potentiodynamic polarization curves of the CL1 and CL2 samples are given in Figure 3.10. The Tafel extrapolation method was used to obtain the corrosion current densities. Ecorr, Icorr and corrosion rate of the samples are given in Table 3.1.

Compared to the CL1 sample, the highest corrosion rate was obtained with S3 with 3670 mpy. This is followed by S2 and S1 with 2820 and 2620 mpy values, respectively. As for the CL2 samples, S2 shows a lower corrosion rate of 1040 mpy compared to S1 and S3, which have 1110 and 1560 mpy, respectively. CL2 sample has higher corrosion resistance than CL1. In addition, the corrosion resistance values change according to the change in the microstructure of the riveted material sections. The shape grain of the materials is changed by the plastic deformation of the mechanical riveting.

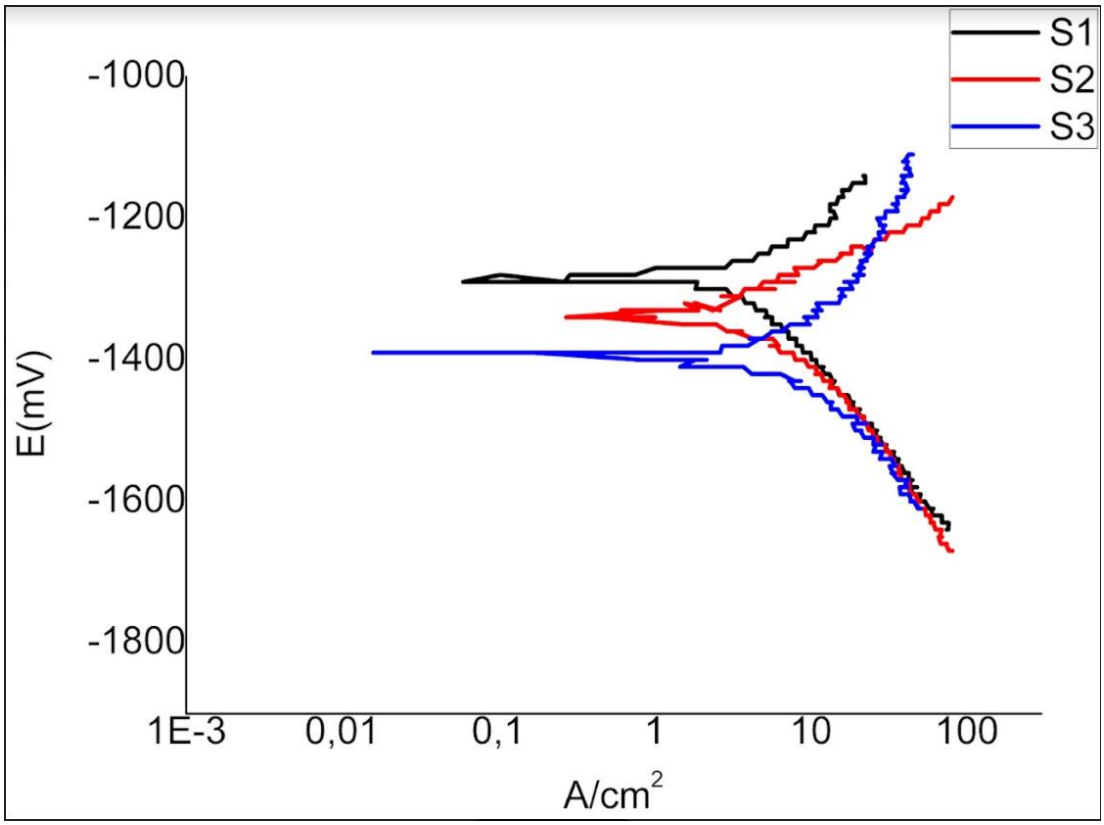

Figure 3. 11. Potentiodynamic Tafel curves obtained from S1, S2 and S3 sections of clinched IF-AZ31B-0.5Nd-0.1La

It is reported that the lower corrosion rate in Mg alloys can be achieved by microstructure without a secondary phase. The dense boundary of secondary phases aggravates the corrosion attacks due to the galvanic corrosion. Grain size dependent segregation also influences the corrosion rate, where the finer grains diminish the segregation, which is more homogeneously continued because of fine grained microstructure. The combined effect of twins fraction and grain size as well as

volume fraction deteriorate the corrosion performance S1 section of AZ31B considerably. Moreover, the volume fraction of secondary phases of S2 and S3 section of AZ31B predominantly got worse the corrosion resistance, where dense smaller secondary phases resulting from fragmentation during rolling give rise to galvanic corrosion attacks [10]. On the other hand, the observed small particles of AZ31B-0.5Nd-0.1La which is a fragment of secondary phases embedded in matrix less than AZ31B resulting in better corrosion resistance. while the S1 section of AZ31B-0.5Nd-0.1La has smaller secondary phases imparting to rising corrosion rate which demonstrates the dominant mechanism is the volume fraction effect for corrosion resistance. To achieve the best corrosion resistance the high-volume fraction of the secondary phase is necessary, but the balanced finer grain with larger sized secondary phases is effective to enhance corrosion resistance [9].

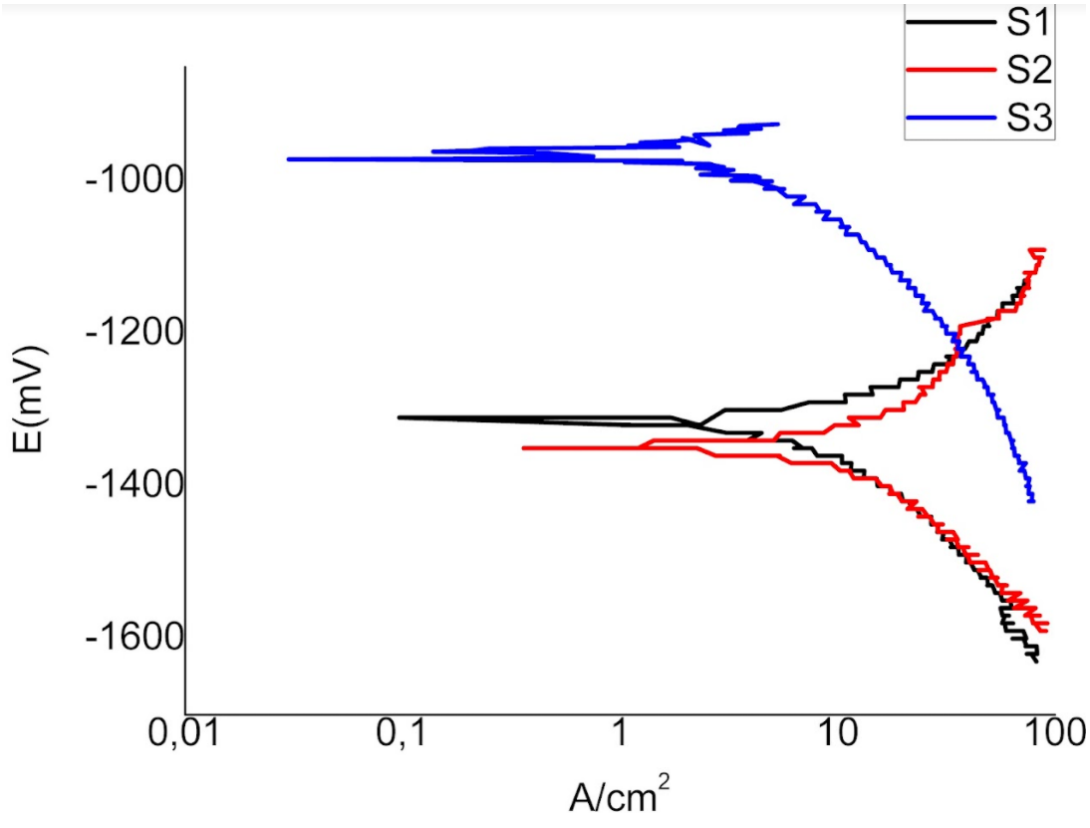

Figure 3. 12. Potentiodynamic Tafel curves obtained from S1, S2 and S3 sections of clinched IF-AZ31B-0.5Nd-0.2La

Figure 3.12. shows the potentiodynamic corrosion curves of clinched IF-AZ31-0.5Nd-0.2La materials. The table also illustrates the Ecorr values of the section of

clinched IF-AZ31-0.5Nd-0.2La materials. It is seen that the closest region to positive volt is S3 and it is followed by S1 and S2. Moreover, the corrosion rate of S2 is higher than the other locations of S1 and S3. The lowest corrosion rate was obtained by the location of S3.

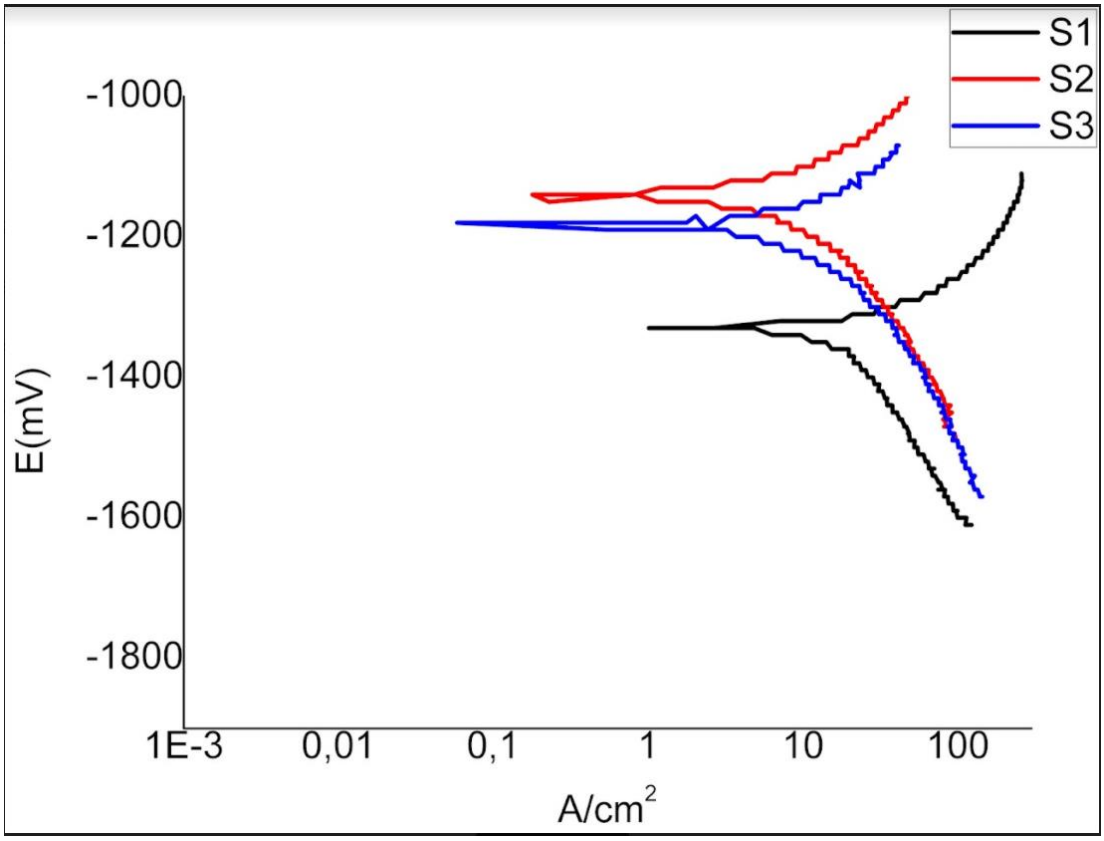

Figure 3. 13. Potentiodynamic Tafel curves obtained from S1, S2 and S3 sections of clinched IF-AZ31B-0.5Nd-0.5La

Figure 3.13. demonstrates the potentiodynamic corrosion curves of clinched IF-AZ31-0.5Nd-0.5La sheets. The table also illustrates the Ecorr values of the section of clinched IF-AZ31-0.5Nd-0.5La sheets. It is observed that the closest region to positive volt is S2 and it is followed by S3 and S1. Moreover, the corrosion rate of S1 is higher than the other locations of S3 and S1. The lowest corrosion rate was obtained by the S2 location of clinched IF-AZ31-0.5Nd-0.5La sheets.

3.1.3. Immersion Corrosion Test

Table 3.2. shows the immersion tests results in 3.5% NaCl solution at 25°C. As seen in the table the metal loss of clinched materials during immersion test is increasing by the rising of test duration. However, the metal loss comparison at 4 hours immersion time illustrates that the IF-AZ31 and IF-AZ31-0.5Nd-0.1La is similar. When we compare the metal loss of IF-AZ31-0.5Nd-0.2La and IF-AZ31-0.5Nd-0.5La with IF-AZ31, the IF-AZ31 is more resistant to corrosion environment than IF-AZ31-0.5Nd-0.2La, whereas IF-AZ31-0.5Nd-0.5La showed less metal loss than IF-AZ31. As to 8 hours duration, IF-AZ31 belongs to the lowest metal loss value in the clinched joints. However, immersion duration of 16 hours demonstrates that the best corrosion resistance is given by IF-AZ31-0.5Nd-0.5La joining and the corrosion resistance can be ordered as IF-AZ31-0.5Nd-0.5La> IF-AZ31-0.5Nd-0.1La> IF-AZ31> IF-AZ31-0.5Nd-0.2La. Fig. presents after 8 hours the metal loss inclination is rising with IF-AZ31-0.5Nd-0.2La extremely and then decreasing through IF-AZ31-0.5Nd-0.5La . It can be said that the metal loss speed of 16 hours duration parameter, the highest point is measured by IF-AZ31-0.5Nd-0.2La, however the lowest point is determined with IF-AZ31-0.5Nd-0.5La.

Table 3. 2. Metal loss values during immersion test (g).

Clinched Materials	4 hours	8 hours	16 hours
IF-AZ31	0.27	0.40	1.09
IF-AZ31-0.5Nd-0.1La	0.27	0.59	1.08
IF-AZ31-0.5Nd-0.2La	0.31	0.63	1.25
IF-AZ31-0.5Nd-0.5La	0.26	0.52	0.79

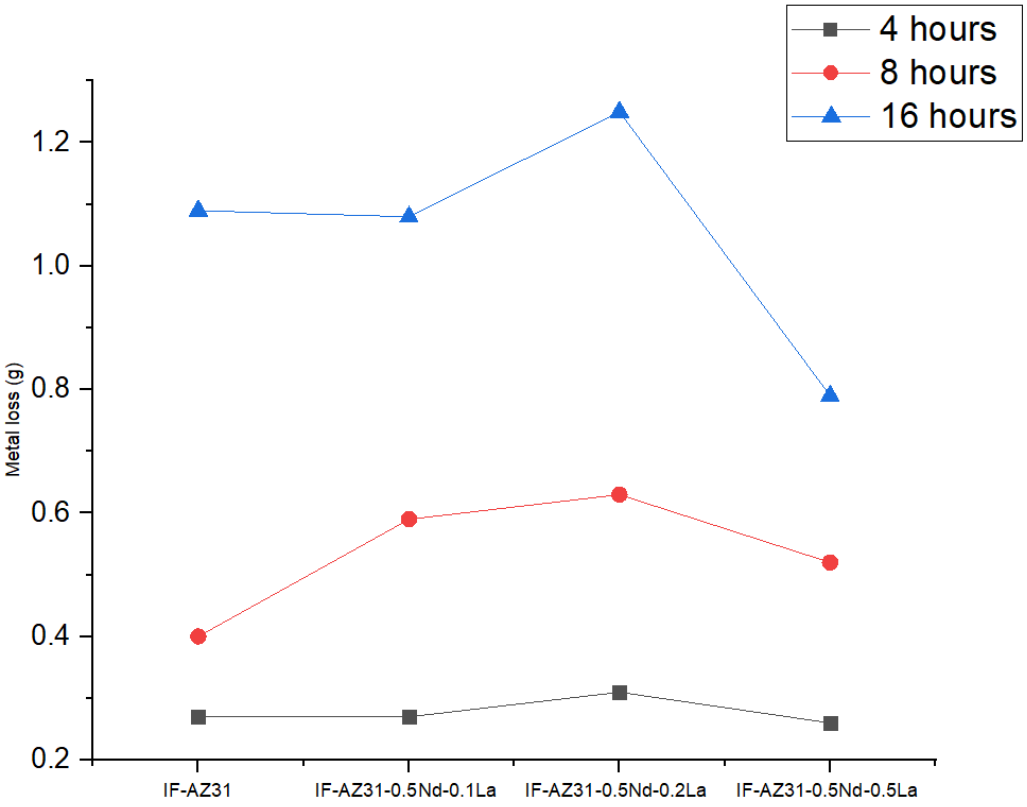

Figure 3. 14. The Metal loss of joined materials during immersion corrosion test.

PART 4

CONCLUSIONS

The microstructure results showed that the addition of both Nd and La changed the orientation of grains of AZ31 Mg alloys during the mechanical clinching process due to the formation of secondary phases including Nd and La which distributed on the grain boundaries and in the grains of AZ31-0.5Nd-(0.1-0.5) La alloys. The rising of La addition in the composition of AZ31 influenced the corrosion rate positively in the amount of %wt.0.2La. however, the corrosion resistance was changed as negatively when the amount of La is wt.%0.2 and wt.%0.5. the different locations of investigated joined materials showed that the different corrosion resistance based on both grain orientations and secondary phases distributions as well as their volumetric fractions. The best corrosion resistance was obtained by the clinched IF-AZ31-0.5Nd-0.2La alloys with the location of S3 which has the value of 989mpy. However, the lowest corrosion resistance was measured as 124900 mpy value with clinched IF-AZ31-0.5Nd-0.2La alloys of S2 location. IF-AZ31-0.5Nd-0.1La alloys possess the lower corrosion rate than IF-AZ31 for all location of clinched regions. The immersion corrosion test of investigated materials shows the combined effect of location of clinched parts containing S1, S2 and S3 locations.

REFERENCES

1 N. N. Aung and W. Zhou, "Effect of grain size and twins on corrosion behaviour of AZ31B magnesium alloy," ***Corrosion Science***, 52, p.p 589-594, (2010).

2 X. He, L. Zhao, H. Yang, B. Xing, Y. Wang, C. Deng, F. Gu and A. Ball, "Investigations of strength and energy absorption of clinched joints," ***Computational Materials Science***, p.p 58-65, (2014).

3 S. Prasad Narla, R. Narasimhan and S. Suwas, "Role of Tensile Twinning on Fracture Behavior of Magnesium AZ31 Alloy," ***Magnesium Technology***, p.p 145-150, (2015).

4 K. Hono, C. Mendis, T. Sasaki and K. Oh-Ishi, "Towards the development of heat-treatable high-strength wrought Mg alloys," ***Scripta Materialia***, 63, p.p 710-715, (2010).

5 X. Liu, B. Zhu, C. Xie, J. Zhang, C. Tang and Y. Chen, "Twinning, dynamic recrystallization, and crack in AZ31 magnesium alloy during high strain rate plane strain compression across a wide temperature," ***Materials Science and Engineering: A***, 733, p.p. 98-107, (2018).

6 R. Neugebauer, S. Dietrich and C. Kraus, "Dieless clinching and dieless rivet-clinching of magnesium," ***Key Engineering Materials*** , p.p 693-698, (2007).

7 M. K. Sabra Atia and M. K. Jain, "Die-less clinching process and joint strength of AA7075 aluminum joints," ***Thin-Walled Structures***, 120, p.p 421-431, (2017).

8 V. Babalo, A. Fazli and M. Soltanpour, "Electro-Hydraulic Clinching: A novel high speed joining process," ***Journal of Manufacturing Processes***, p.p 559-569, (2018).

9 İ. H. Kara, H. Ahlatcı, Y. Türen and Y. Sun, "Microstructure and corrosion properties of lanthanum-added AZ31 Mg alloys," ***Arabian Journal of Geosciences***, 11, p. p 535, (2018).

10 L.-l. Guo and F. Fujita, "Effect of deformation mode, dynamic recrystallization and twinning on rolling texture evolution of AZ31 magnesium alloys,"

Transactions of Nonferrous Metals Society of China, 28, p.p 1094-1102, (2018).

11 D. Yin, K. Zhang, G. Wang and W. Han, "Warm deformation behavior of hot-rolled AZ31 Mg alloy," ***Materials Science and Engineering A***, 392, p. p 320-325, (2005).

12 L. Shang, *Effect of Micro Alloying on Microstructure and Hot Working Behavior for AZ31 Based Magnesium Alloy*, Montreal, Quebec, Canada : McGill University , (2008).

13 W. Zhang, K. Li, R. Chi, S. Tan and P. Li, "Insights into microstructural evolution and deformation behaviors of a gradient textured AZ31B Mg alloy plate under hypervelocity impact," ***Journal of Materials Science & Technology***, 91, p.p 40-57, (2021).

14 L. Di, L. Zuyan and W. Erde, "Effect of rolling reduction on microstructure, texture, mechanical properties and mechanical anisotropy of AZ31 magnesium alloys," ***Materials Science and Engineering: A***, 612, p.p 208-213, (2014).

15 Zhang, H. Hao, X. Liu and X. Zhang, "Effects of precipitates on grain size and mechanical properties of AZ31-x%Nd magnesium alloy," ***Journal of Rare Earths***, 32, p. p 451-457, (2014).

16 M. Li, C. Li, X. Liu and B. Xu, "Effect of Nd on Microstructure and Mechanical Properties of AZ31 Magnesium Alloy," ***Rare Metal Materials and Engineering*** 38, p. p 7-10, (2009).

17 S. Li, W. Zheng, B. Tang, D. Zeng and X. Guo, "Grain Coarsening Behavior of Mg-Al Alloys with Mischmetal Addition," ***Journal of rare earths***, 25, p. p 227-232, (2007).

18 L. Shang, I. Jung, S. Yue, R. Verna and E. Essadigi, "An investigation of formation of second phases in microalloyed,AZ31 Mg alloys with Ca,Sr and Ce," ***Journal of Alloys and Compounds***, 492, p. p 173-783, (2010).

RESUME

Ziadoon Tareq Mhawesh MHAWESH graduated first and elementary education in this Iraq. He completed high school education in EL Hussein High School, after that, he started undergraduate program in University of Technology - Department of Production Engineering and Metallurgy in 1998. Then in 2002, I started working in one of the companies of the Ministry of Industry and Minerals as an engineer in the production department.